



# Effect of die design parameters on the deformation behavior in pure shear extrusion



F. Rahimi<sup>a</sup>, A.R. Eivani<sup>a,\*</sup>, M. Kiani<sup>b</sup>

<sup>a</sup> School of Metallurgy and Materials Engineering, Iran University of Science and Technology (IUST), Tehran, Iran

<sup>b</sup> Department of Materials Engineering, Science and Research Branch, Islamic Azad University, Kermanshah, Iran

## ARTICLE INFO

### Article history:

Received 9 February 2015

Revised 31 May 2015

Accepted 4 June 2015

### Keywords:

Finite element method

Pure shear extrusion

Strain distribution

Filling fraction

Pressing load

## ABSTRACT

Influences of die design parameters in terms of diameter ratio and length of the deformation zone on the distribution of effective strain, filling fraction of the die exit channel and pressing load in pure shear extrusion (PSE) are studied using finite element method (FEM). Dimensional stability, pressing load and hardness measurements are used to validate the predictions of the simulation. Acceptable agreements between the predictions of simulation and experimental results are observed. It is found that strain is inhomogeneously distributed which increases from the center to the corners. Effective strain, inhomogeneity of strain, filling fraction of the die exit channel and pressing load are increased with increasing diameter ratio. In addition, the work-piece is deformed more homogeneously at lower pressing load by increasing the length of deformation zone. However, filling fraction of the die exit channel initially increases by the length of the deformation zone up to 60 mm after which it reduces. The optimum die design parameters covering a range of acceptable effective strain and strain homogeneity, filling fraction of the die exit channel and pressing load are proposed as being 60 mm and 2 for length of the deformation zone and diameter ratio, respectively.

© 2015 Elsevier Ltd. All rights reserved.

## 1. Introduction

The grain structure of an engineering material is an important factor which can significantly influence its physical and mechanical properties [1–3]. In this regard, it is demonstrated that materials with submicron or nanoscale grain structures indicate superior properties [4]. Therefore, it is necessary to use an appropriate technique to acquire the highest possible level of grain refinement [5]. In recent years, severe plastic deformation (SPD) has been used as an appropriate technique for grain refinement in bulk materials and consequently enhancement of the material properties [6–8].

So far, the most widely used methods for SPD processing are accumulative roll bonding (ARB) [9], high pressure torsion (HPT) [10,11], equal channel angular pressing (ECAP) [12–15], twist extrusion (TE) [16] and constrained groove pressing (CGP) [17]. Some of these laboratory scale techniques have been recently developed for industrial applications [18]. In addition, simple shear extrusion (SSE) has been recently introduced by Pardis and Ebrahimi [19], which serves as a new SPD technique for gradual deformation of the samples in simple shear mode [19].

A new SPD technique based on pure shear, i.e., pure shear extrusion (PSE), has been recently introduced by the present authors [20,21]. Pure shear is the dominant deformation mode of the material in this method. Application of a different mode of deformation may significantly affect the evolution of microstructure as claimed by Segal [22]. In fact, pure shear deformation in PSE is considered as a new achievement in PSE vs. simple shear which is the main deformation mode in most of the known SPD techniques, e.g., ECAP, TE and SSE.

Homogeneity of deformation is another key factor determining the effectiveness of a SPD process. In fact, a SPD process may be considered efficient if the deformation and consequently the improvement in mechanical properties are uniform. According to previous studies, it is well understood that some SPD techniques such as HPT and TE are inherently involved with inhomogeneous deformation [23,24]. However, the level of inhomogeneity changes with process parameters. For example, it is observed that by increasing the number of rotations in HPT, the homogeneity in hardness is improved [25]. Akbari Mousavi et al. [26] reported that with employing direct extrusion in TE, the sample is deformed more homogeneously. Moreover, by repeating the TE for further cycles, the hardness of the processed sample is distributed more uniformly [27]. It is worth mentioning that the proper amount of back pressure and modified frictional condition have significant effects on

\* Corresponding author.

E-mail address: [aeivani@iust.ac.ir](mailto:aeivani@iust.ac.ir) (A.R. Eivani).

the distribution of strain in TE [16]. Regarding the ECAP process, it is observed that enhancement of the intersecting angle of the two channels increases the uniformity of deformation [28]. Wang et al. [29] reported that by employing the modified die design, samples may be deformed for more cycles without formation of major imperfections such as cracks and higher level of grain refinement with the optimum uniformity may be achieved. In addition, Djavanroodi et al. [30] used copper tube casing (CTC) method to increase the uniformity of the deformation across the sample in ECAP. It is observed that the strain inhomogeneity decreases as the cover tube thickness increases. Moreover, it is found that friction and back pressure may affect the homogeneity of deformation. In fact, Yoon et al. [31] observed that lower friction leads to the most uniform deformation while back pressure is applied during processing in ECAP. It should be added that the outer corner radius of the intersecting channel in ECAP has a noteworthy effect on the material flow and the strain inhomogeneity after deformation [32]. Kazeminezhad et al. [33] investigated the effect of die design in CGP on the deformation behavior of the processed sheet and reported that by processing for more cycles, the uniformity of deformation improves. According to this introduction, one may understand the significance of process parameters, e.g., die design factors, on the homogeneity of deformation in all SPD techniques including the one introduced recently, i.e., PSE [20,21].

This paper is focused on investigating the effect of die design parameters toward acquiring homogeneous deformation throughout the cross section of the product. This is in addition to the fact that the process must be designed to impose the largest strain on the sample. This may provide the opportunity of producing nanostructured materials with homogeneous distribution of nano-sized grains. For this purpose, finite element method (FEM) simulation is used to investigate the effective die design parameters on strain distribution and homogeneity of deformation in the work-piece during PSE. In order to verify the accuracy of the predictions of FEM simulations, experimental investigation was carried out.

## 2. Principles of pure shear extrusion

Principles of PSE are extensively discussed in earlier works of the authors [20,21]. In brief, the work-piece is squeezed through

a channel consisting of five zones as demonstrated in Fig. 1. In the entry channel (zone I), the work-piece experiences no deformation and is directed to move toward the deformation zone. In the upper deformation zone (UDZ) (zone II), the work-piece deforms gradually while its square cross section changes to a rhombic. A diameter ratio of  $D_R$  is defined as the ratio between the largest diameter of the rhombic to that of square, as shown in Fig. 1. One may note that during the deformation, the cross sectional area of the work-piece remains unchanged. The use of relaxation zone (RZ) (zone III) at which no deformation is imposed on the work-piece is optional, but it may be effective on the filling fraction of the die and homogeneity of deformation. In Zone IV, the lower deformation zone (LDZ), shear deformation is imposed but in an opposite direction to that at zone II. This causes the work-piece to return back to its initial square cross sectional shape, i.e., from rhombic to square. In the exit channel (zone V), precisely similar to zone I, the work-piece experiences no deformation and finds the way out of the die.

The gradual changes in the cross sectional shape of the work-piece is schematically illustrated in Fig. 1. Since there is no change in the cross sectional area of the work-piece, there would be no enlargement of the work-piece. Consequently, by reversing the imposed deformation on the work-piece in zone IV, it is possible to return the sample back into its initial geometry. This method allows repetition of the process for several times and achieve higher strain which is the major key condition for a SPD technique.

## 3. Experimental procedure

Billets, 120 mm in length with square cross section of  $20 \times 20 \text{ mm}^2$  were cut out from rolled sheets of aluminum AA1050. Chemical composition of the alloy is presented in Table 1. The samples were annealed at  $550 \text{ }^\circ\text{C}$  for 30 min and cooled to room temperature in furnace. PSE experiments were performed at room temperature using a hydraulic press with ram speed of  $1 \text{ mm s}^{-1}$  and pressing load was recorded. In order to reduce friction between the work-piece and the die walls, molybdenum disulfide ( $\text{MoS}_2$ ) was used as lubricant. The experiments were stopped when the work-piece was totally extruded. In order to investigate the uniformity of the strain distribution and the

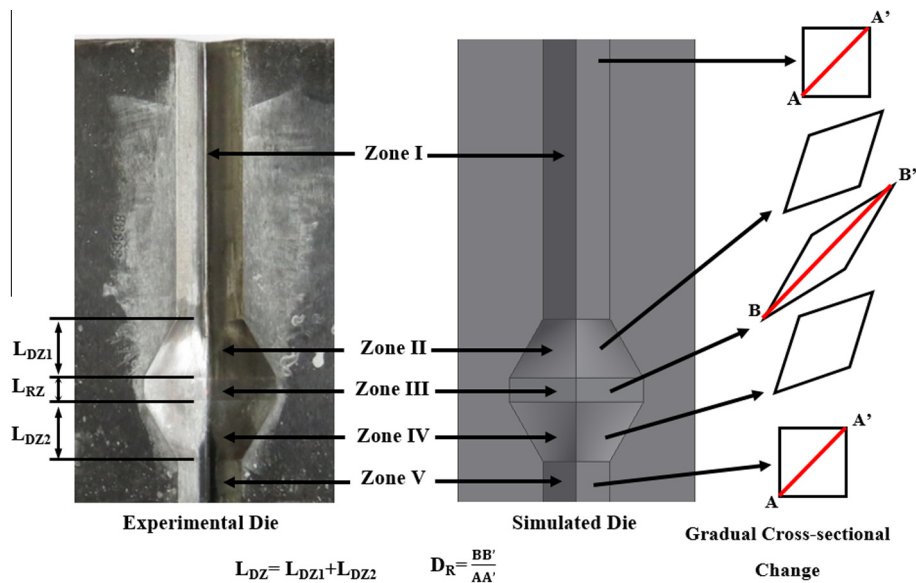


Fig. 1. Schematic illustration of pure shear extrusion (PSE), depicting the die consisting of five zones; gradual changes in the cross-sectional shape throughout the die, diameter ratio ( $D_R$ ) and lengths of deformation zone ( $L_{DZ}$ ) and relaxation zone ( $L_{RZ}$ ).

**Table 1**  
Chemical composition of AA1050 aluminum alloy (wt.%).

Al	Si	Na	Fe	Ca	Cr	Pb	Zn	Sn	Ni	Zr	Ti	Bi
Balance	0.124	0.002	0.252	0.001	0.001	0.002	0.014	0.005	0.004	0.001	0.003	0.001

homogeneity of deformation in the work-piece, microhardness measurements were performed on the normal plane of the sample to the extrusion direction in the exit channel. The measurements were performed using Vickers approach by means of Bohler microhardness testing equipment with an applied load of 50 gf for 15 s.

#### 4. Material modeling and simulation procedure

The commercial finite element method (FEM) package, DEFORM 3D™, was used to carry out the simulation of the deformation. The punch and the die were modeled as rigid bodies. Variations of the length of deformation zone ( $L_{DZ}$ ) i.e., the length of zones II and IV, relaxation zone ( $L_{RZ}$ ) and diameter ratio ( $D_R$ ), as shown in Fig. 1, are subjected to study and varied as shown in Table 2.

The work-piece was considered as a sample with square cross section and dimensions of  $20 \times 20 \times 120 \text{ mm}^3$  with 35,000 tetrahedral elements. Material characteristics that were implemented in the simulation are defined according to the software manual and depicted as in Eq. (1) [34]:

$$\bar{\sigma} = \bar{\sigma}(\bar{\epsilon}, \dot{\bar{\epsilon}}, T) \quad (1)$$

where  $\bar{\sigma}$  is the flow stress,  $\bar{\epsilon}$ , the effective strain,  $\dot{\bar{\epsilon}}$ , the effective strain rate and  $T$ , the temperature which remains constant at 20 °C in the course of deformation.

Commercially pure aluminum alloy was used as the billet material. The friction condition between the surface of the work-piece, die and punch were considered as shear type. Simulations were run with coefficients of 0.1–0.6 with increments of 0.1 to determine the proper shear friction coefficient ( $m$ ) with the highest accordance between the results of simulations and experiments. All computer simulations were performed at a punch speed of  $1 \text{ mm s}^{-1}$  at isothermal condition.

Predictions of simulation were analyzed in terms of value and inhomogeneity of strain, filling fraction and pressing load. In order to investigate the inhomogeneity of strain and deformation, standard deviation ( $S.D.$ ) is used as presented in Eq. (2) [30]:

$$S.D. = \sqrt{\frac{\sum_{i=1}^N (\epsilon_i - \epsilon_{avg})^2}{N - 1}} \quad (2)$$

where  $\epsilon_{avg}$  is the average effective strain,  $\epsilon_i$ , the effective strain for the  $i$ -th point and  $N$ , the total number of points. One may note that more homogenous deformation may be achieved at smaller  $S.D.$  values.

Filling fraction ( $F_f$ ) is calculated using Eq. (3):

$$F_f = \frac{S_W}{S_C} \times 100 \quad (3)$$

where  $S_W$  is the cross sectional area of the work-piece which fills in the die channel and  $S_C$ , cross sectional area of the die channel at any normal plane to the extrusion direction.

**Table 2**  
Variation of die design parameters subjected to study in this investigation.

Design parameters											
Diameter ratio			$L_{DZ}$ (mm)						$L_{RZ}$ (mm)		
1.5	2	2.5	30	40	50	60	70	80	90	10	

## 5. Results and discussion

### 5.1. Deformation of a sample in PSE

#### 5.1.1. Pressing load

Variation of applied load versus punch displacement is illustrated in Fig. 2. The pressing load curve can be divided into six different regions indicated by alphabetical letters. It is clear that two hills and one plateau is formed in the pressing load graph. The initial increase in the pressing load curve (points O to A) is related to the easy movement of the work-piece through the die channel. It is observed that after point A, the pressing load is slightly reduced (points A to B) which may be correlated to the fact that at the initial stage of the work-piece movement, a static frictional condition is exerted. However, as the deformation continues, a dynamic frictional condition is applied which results in a minor reduction in pressing load. Considering the length of the UDZ in the die set up used in this investigation, one may understand that the hill formation in the graph (points O to C) is related to the deformation of the work-piece in the UDZ. As the sample enters the UDZ and starts to deform, more internal energy is consumed and the frictional contact area slightly increases. Therefore, an increase in the pressing load is observed. This gradual increase in pressing load continues to punch displacement of 40 mm at which the RZ begins (point C). When the sample enters the RZ, applied load is almost unchanged which is correlated to the fact that no deformation is occurring and the contact area is almost unchanged (points C to D). By further increase in the punch displacement, the sample enters the LDZ. As the deforming sample moves through this zone, it deforms which results in enhancement of contact areas as well as continuation of deformation. Therefore, the second hill is observed in the pressing load curve (points D to E). As the work-piece moves through the die exit channel, pressing load decreases (points E to F) which is correlated to reduction of contact area between the deforming sample and the die wall, as it is not fully filling in the die exit channel.

#### 5.1.2. Filling fraction

Changes in the geometry of a sample in the course of PSE deformation, i.e., before entering into, inside and after leaving the

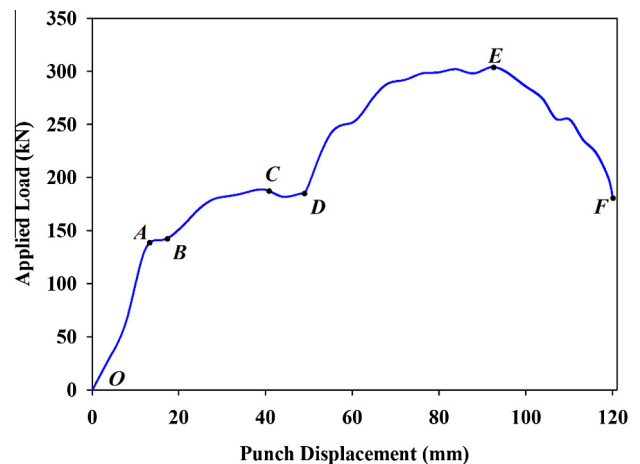


**Fig. 2.** Variation of applied load versus punch displacement.

deformation zone is shown in Fig. 3(a). It is clear that the sample has not fully filled in the deformation zone and gaps are formed at the edges of the sample as indicated by circles. The cross section of the sample at the die exit channel on a normal plane to extrusion direction is shown in Fig. 3(b). It is clear that sharp and curved corners are formed. Ideally, the work-piece should completely shear inside the deformation zone and totally fill in the die channels during deformation in PSE which has not obviously occurred. In fact, the sample is not totally returned to its initial shape and does not fully fill in the die exit channel. Lots of energy must be consumed during deformation to shear the sample and force it to slide against frictional surfaces. The level of shear deformation and contact frictional surfaces increase by continuation of deformation. If the sample does not fully fill in the die channel, less energy would be consumed and since the bottom side of the deformation channel is free, the sample moves to exit with less deformation. In such a case, the sample moves straight with the least contact with the die walls instead of consuming high frictional energy due to the contact between the sample and the die walls. Consequently, corner gaps form as demonstrated in Fig. 3(b).

5.2. Verification of the simulation

5.2.1. Pressing load

Predicted applied load versus punch displacement at various values of shear friction coefficient ( $m$ ) is used in order to validate the predictions of the model. For this purpose, simulation is run at various  $m$  and the predicted pressing load is compared with the experimental results in Fig. 4. It can be seen that a reasonable agreement between the predictions of simulation and experimentally measured pressing load is obtained at  $m$  equal to 0.4.

5.2.2. Filling fraction

Effect of  $m$  on the filling fraction of the die exit channel is illustrated in Fig. 5(a). It is clear that with increasing  $m$ , the filling fraction increases. This may be correlated to the fact that the large value for  $m$  indicates a high opposite force against the movement of the work-piece during deformation. This opposite force acts similar to backward pressure and forces the sample to more

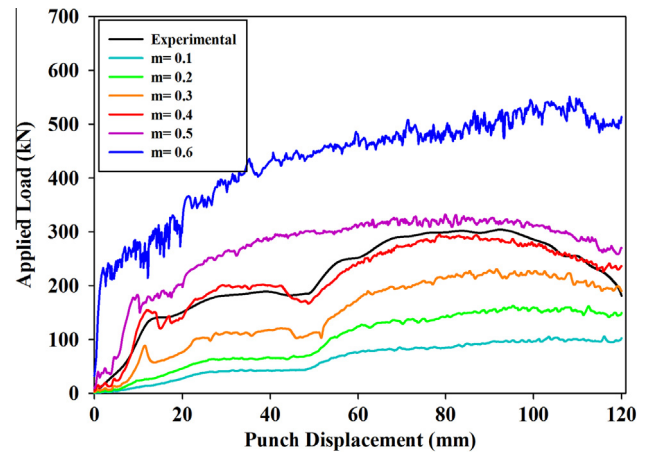


Fig. 4. Variation of applied load versus punch displacement in FEA and Experiment.

significantly fill in the die exit channel. This is in line with the earlier findings of Djavanroodi and Ebrahimi in ECAP processing [35].

In Fig. 5(b), the filling fraction of the die exit channel at various  $m$  is compared to experimental results for a die with  $D_R$  of 2 and  $L_{RZ}$  and  $L_{DZ}$  of 10 and 50 mm, respectively. It is clear that a good agreement between the predictions of simulation and the experimental results is found at 0.4. This is in line with  $m$  value of 0.4 obtained from the comparison between the previously predicted pressing loads and the experimental results in Fig. 4.

5.2.3. Strain distribution

Hardness of the work-piece is measured 1 mm underneath LDZ, on a normal plane to the extrusion direction in order to evaluate the homogeneity of strain distribution and verify the predictions of simulation. Fig. 6(a) exhibits the color coded map of hardness on the mentioned plane. It is clear that the Vickers microhardness increases from periphery to the center of the work-piece. Since hardness increases due to work hardening which by itself is affected by the value of plastic strain, it can be concluded that the peripheral regions experience higher strain resulting in more

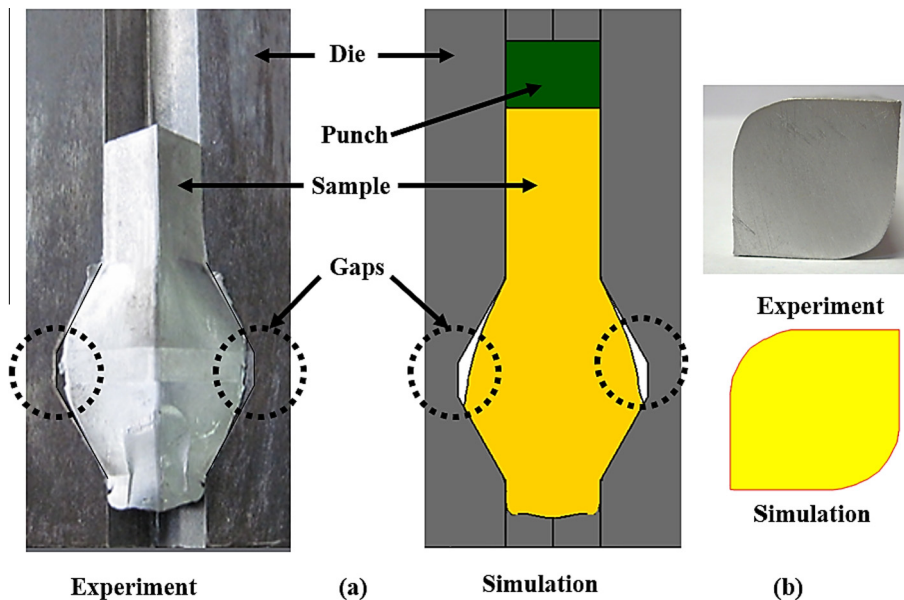


Fig. 3. (a) Changes in the geometry of the sample during PSE leading to the formation of corner gaps (left) experimental and (right) FEM predictions and (b) formed corner gaps in the die exit channel after one pass PSE, (upper) experimental and (lower) predictions of simulation.

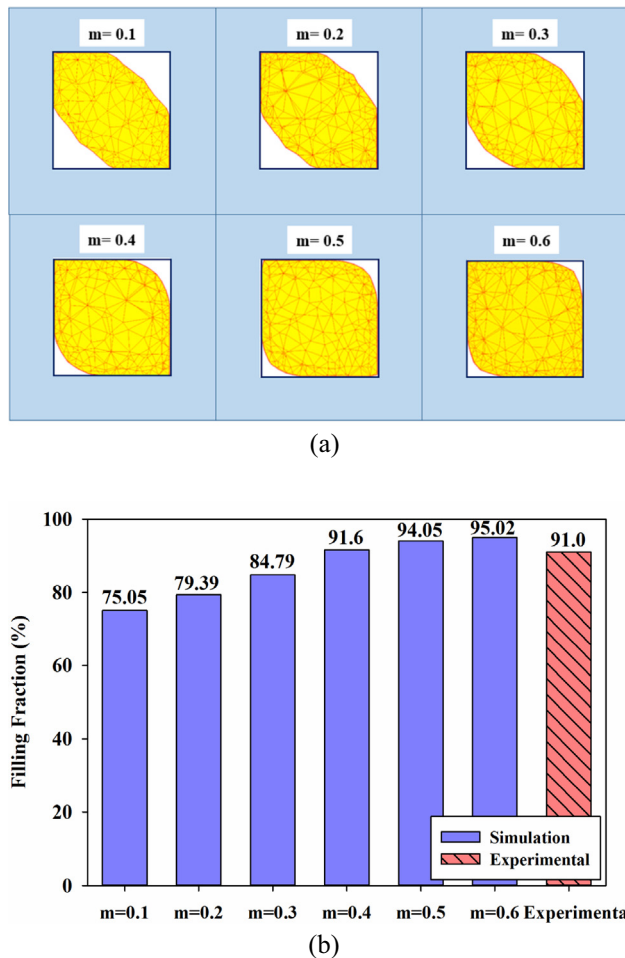


Fig. 5. (a) Effect of  $m$  on the evolution of sample shape in the die exit channel, and (b) comparison between experimentally measured values for filling fraction and the predicted values at various  $m$ .

work hardening and obtaining higher microhardness. The predicted distribution of strain in the cross section of the sample after one pass PSE in the die exit channel is shown in Fig. 6(b). It should be noted that this prediction is taken from the similar plane as that on which hardness was measured (for Fig. 6(a)) and is not necessarily similar to the plane in Figs. 7 or 11. It can be seen that strain is higher at the sharp edges and reduces by increasing distance from the edges toward the center. It is clear that an acceptable agreement between the predictions of simulation for distribution of strain and experimentally measured distribution of hardness is observed.

### 5.3. Predictions of the model

#### 5.3.1. Effect of diameter ratio

5.3.1.1. *On strain distribution.* Fig. 7 shows the distribution of effective strain at different values of diameter ratio ( $D_R$ ). For this set of predictions,  $D_R$  ranged from 1.5, 2 and 2.5 and  $L_{DZ}$  and  $L_{RZ}$  were considered constant, 50 and 10 mm, respectively. As explained earlier, while the sample moves through the deformation zone, it spreads in one diagonal while shrinks in the other one, i.e., square cross section changes to rhombic. The strain contours in the deformation zone on the long diagonal of the rhombic are shown in Fig. 7(a). It is clear that strain is inhomogeneously distributed. Since the homogeneity of strain at the final stage when deformation is

finished is more interesting in a deformation process, the distribution of effective strain on a plane normal to the extrusion direction in the deformed work-piece is investigated which is shown in Fig. 7(b). It is clear that similar to the course of deformation shown in Fig. 7(a), the inhomogeneity of strain remains in the processed material. In addition, sharp corners experience the largest strain. This may be correlated to frictional condition between the surface of the work-piece and the die walls causing severe deformation of the material at the surface. In addition, formation of corner gaps may be observed in all  $D_R$  values.

Results of the predictions presented in Fig. 7 are quantified which are subjected to more detailed attention in Fig. 8. Variations in effective strain at the cross section of the deformed work-piece alongside the stretching diameter (point A to A' in Fig. 1) are illustrated in Fig. 8(a). One may note that by increasing  $D_R$ , strain enhances. This is due to the fact that more significant elongation and shortening of the long and short axes of the cross section of the rhombic occurs which results in achievement of higher strain. Larger strain of material at the periphery of the work-piece is as well obvious in this figure, which is correlated to the existence of sticking friction between the deforming sample and the die walls.

Fig. 8(b) exhibits the predictions of simulation on the homogeneity of effective strain in the samples as a function of  $D_R$ . For this purpose,  $S.D.$  is calculated using Eq. (2) for 20 points. It is clear that by increasing  $D_R$ ,  $S.D.$  increases which indicates a reduction in the homogeneity of deformation. As a conclusive remark, it can be stated that a large increase in strain occurs by increasing  $D_R$  from 1.5 to 2, while it does not change significantly from 2 to 2.5. In addition, homogeneity of strain reduces nearly linearly by increasing  $D_R$ .

5.3.1.2. *On filling fraction.* Fig. 9 displays the effect of  $D_R$  on the filling fraction ( $F_f$ ) of the die exit channel and the contact area between the deforming sample and the die walls in the deformation zone.  $F_f$  is calculated using Eq. (3). It is observed that by enhancement of  $D_R$ ,  $F_f$  increases. In fact, by increasing  $D_R$ , higher plastic deformation is applied resulting in larger consumption of internal energy and increased pressing load. In addition, the contact area between the work-piece and the die walls increases which results in an increase in the consumption of frictional energy during deformation and further increase in pressing load. Therefore, the easy movement of material throughout the die channels is inhibited and causes the deforming sample to more pronounced filling of the die channel. This is in line with what has been observed in ECAP by Djavanroodi and Ebrahimi [35]. By considering parameters which are affected by  $D_R$ , i.e., strain and filling fraction, it can be concluded that the optimum value for  $D_R$  is 2. At this value, an acceptable filling fraction (see Fig. 9) and relatively large strain (see Fig. 8(a)) with an acceptable homogeneity (see Fig. 8(b)) is obtained.

5.3.1.3. *On pressing load.* The effect of  $D_R$  on the pressing load is illustrated in Fig. 10. It is clear that by increasing  $D_R$ , deformation load increases. Pressing load is affected by two factors. One is the consumption of internal energy in the deformation zone which increases with strain. The second is the consumption of frictional energy on the contact surface between the deforming sample and the die walls. As indicated in Fig. 8(a), strain increases with increasing  $D_R$ . Therefore, more internal energy is consumed for performing larger deformation and an increase in the deformation load is expected. In addition, by increasing  $D_R$ , the sample is forced to deform in a narrower region and move against larger frictional surfaces and consume more energy. Consequently, pressing load increases due to the enhancements in these two parameters.

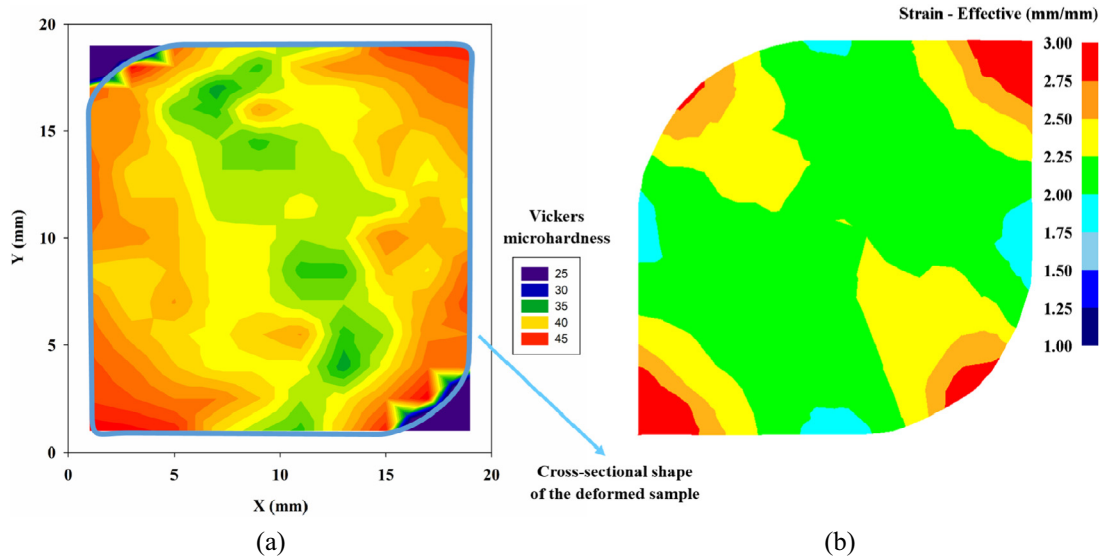


**Fig. 6.** (a) Vickers microhardness color-coded contour map and (b) effective strain contour on a normal plane to the extrusion direction. Both are taken on a plane 1 mm underneath the LDZ. (For interpretation of the references to colour in this figure legend, the reader is referred to the web version of this article.)

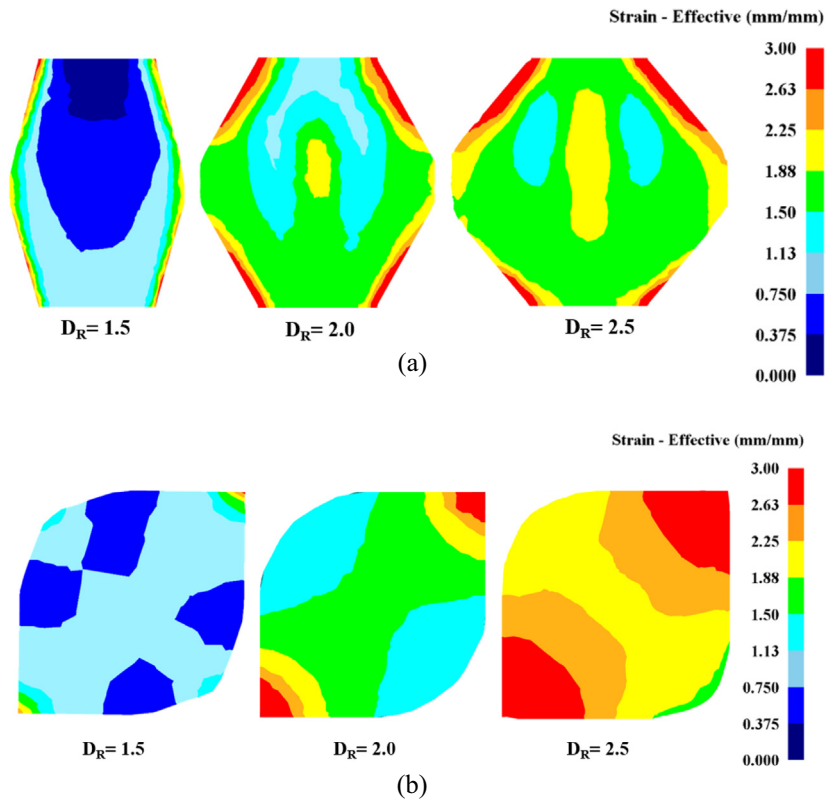


**Fig. 7.** Effective strain contours predicted by FEM in dies with different  $D_R$ , (a) in the deformation zone, and (b) in the die exit channel on a normal plane to extrusion direction.

5.3.2. Effect of the length of deformation zone

5.3.2.1. On strain distribution. FEM predicted effective strain contours on a plane normal to extrusion direction in the deformed work-piece at various values of  $L_{DZ}$  are shown in Fig. 11. The effect of  $L_{DZ}$  on the variation of strain and its homogeneity are shown in Fig. 12. It is clear that by increasing  $L_{DZ}$ , effective strain decreases. This is against what has been previously observed for PSE [21]. It has been previously shown [21] that strain is a sole function of

$D_R$ , and is not a function of  $L_{DZ}$ . One may note that this would be the case if deformation is homogeneous and no corner gap forms. However, the material deforms inhomogeneously and does not fully fill in the die channels and strain is different with the ideal value. In order to explain why strain decreases with  $L_{DZ}$ , it has to be considered that by increasing  $L_{DZ}$ , the sample has to deform in a larger deformation zone and contact areas increase as it is shown in Fig. 13. Consequently, the frictional energy which is consumed

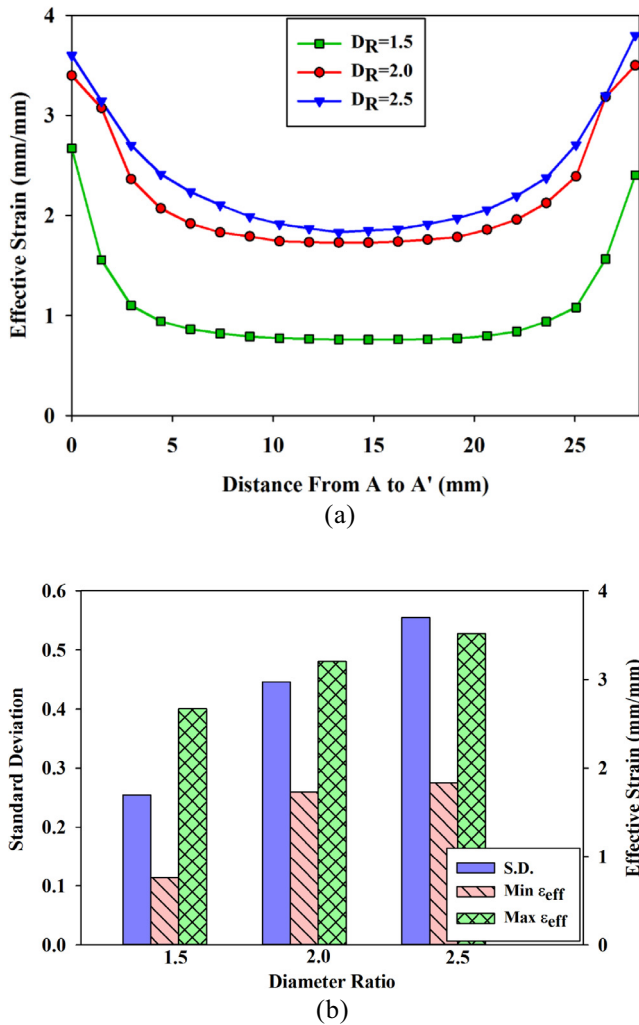


Fig. 8. Effect of  $D_R$  on the (a) variation of effective strain along the stretching diameter of the sample, and (b) inhomogeneity of strain.  $L_{DZ}$  and  $L_{RZ}$  are considered constant, 50 and 10 mm, respectively.

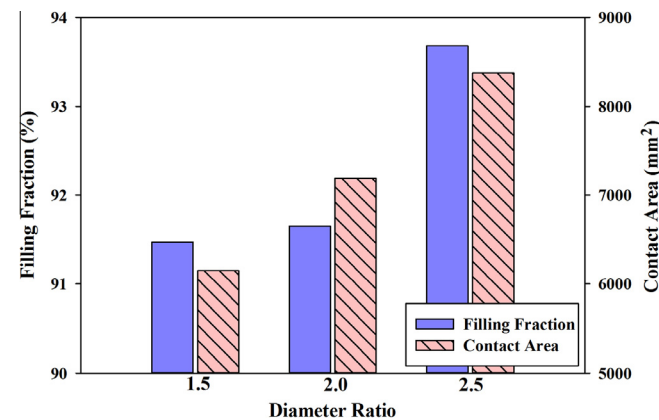


Fig. 9. Effect of  $D_R$  on the filling fraction of the die.  $L_{DZ}$  and  $L_{RZ}$  are considered constant, 50 and 10 mm, respectively.

between the surface of the sample and the die walls increases. At this situation, it is easier for the sample to move directly toward the die exit instead of spreading and being forced to slide against the die walls. Therefore, less deformation and less strain occurs.

According to Fig. 12(b), by enhancement of  $L_{DZ}$ , S.D. reduces which indicates that the material is deformed more homogeneously.

As  $L_{DZ}$  increases at a constant  $D_R$ , the deformation is gradually imposed on the material in a longer deformation zone. This would cause less severe distortion at the surface. Consequently, the difference between the maximum and minimum effective strain and S.D. reduces and deformation would be more homogeneous.

5.3.2.2. On filling fraction. Fig. 13 illustrates the effect of  $L_{DZ}$  on the filling fraction and total possible contact area of the die walls. One may see that by increasing  $L_{DZ}$ , filling fraction increases until it reaches a maximum at  $L_{DZ} = 60$  mm. This is as well correlated to the increased frictional and internal deformation energies acting similar to backward pressure against the movement of the sample and forcing it to fill in the die channels. By increasing  $L_{DZ}$  up to 60 mm, contact area between the sample and the die walls in the deformation zone increases. Therefore, the material is forced to move against frictional surfaces and consume energy and yields pressing load. This increased pressing load in turn forces the sample to shear more significantly and fill in the die channels more pronouncedly. However, as it will be shown in Fig. 13, after the optimum point, i.e.,  $L_{DZ} = 60$  mm, the filling fraction reduces. In fact, 60 mm shows to be the critical value at which consumption of energy on the contact surfaces would exceed the consumption of internal energy for deformation. Therefore, from this point further, the sample reduces its energy consumption by less contact with the die walls and would not fill in the die channel resulting in reduction of filling fraction. This is why the pressing load has reduced by further increase in  $L_{DZ}$ , as shown in Fig. 14.

As a conclusive remark on  $L_{DZ}$ , it should be said that although S.D. continuously reduces by  $L_{DZ}$ , however, at  $L_{DZ} = 60$  mm, the maximum filling fraction is achieved. After this value for  $L_{DZ}$ , the filling fraction reduces which indicates that the sample is not filling in the die channel and is not returning to its initial shape which is essential for an effective SPD process. Therefore, it may be concluded that using a die with  $D_R$  and  $L_{DZ}$  of 2 and 60 mm yields an acceptable high level of strain and force the work-piece to deform more uniformly and return to its initial shape.

5.3.2.3. On pressing load. The effect of  $L_{DZ}$  on pressing load is shown in Fig. 14. It is clear that pressing load is reduced by increasing  $L_{DZ}$ . In order to explain the effect of  $L_{DZ}$  on pressing load, the consumption of internal and frictional energies which play different roles should be considered. Since by increasing  $L_{DZ}$  strain reduces, less consumption of internal energy occurs and reduction in pressing load is expected. As the possible contact area is increased by  $L_{DZ}$ , as shown in Fig. 13, frictional contact area between the work-piece and the die walls is expected to increase. This would have occurred if the sample was fully filling in the die channel.

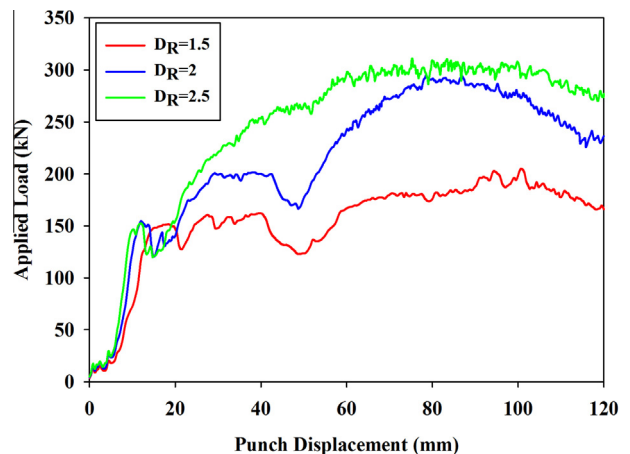


Fig. 10. Effect of  $D_R$  on the pressing load ( $L_{DZ} = 50$  and  $L_{RZ} = 10$  mm).

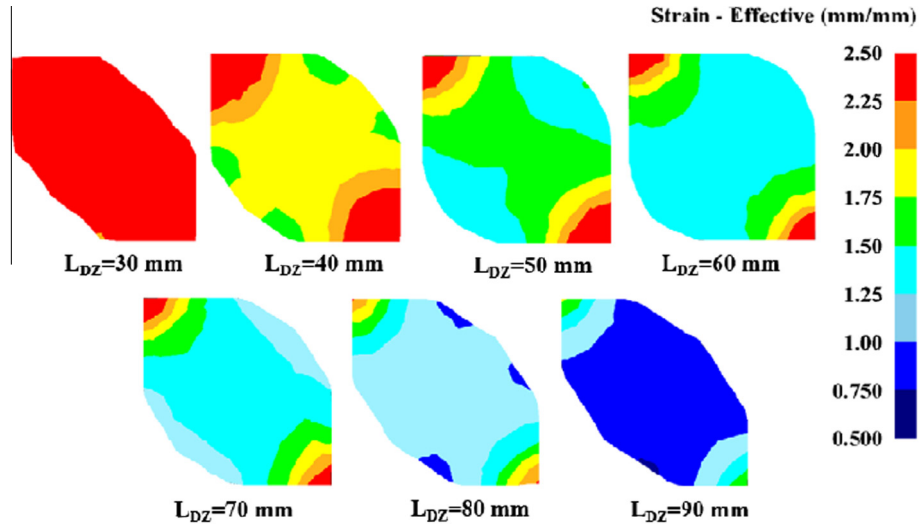
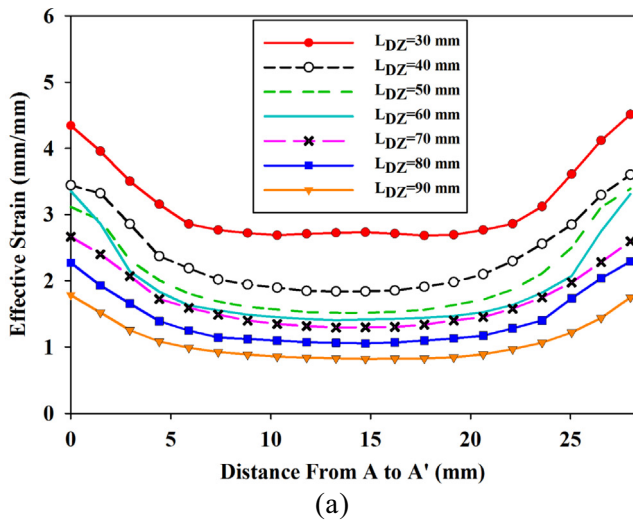
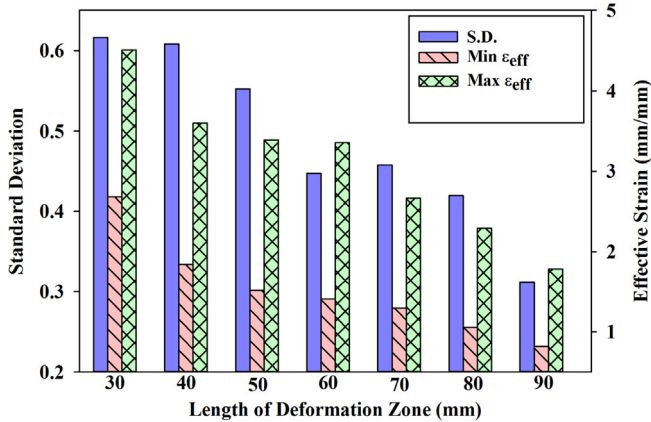


Fig. 11. Effective strain contours predicted by FEM in dies with  $D_R$  of 2 and different  $L_{DZ}$  on a normal plane to extrusion direction.



(a)



(b)

Fig. 12. Effect of  $L_{DZ}$  on the (a) variation of effective strain along the stretching diameter of the sample, and (b) inhomogeneity of strain.  $D_R$  is considered constant and equals 2.

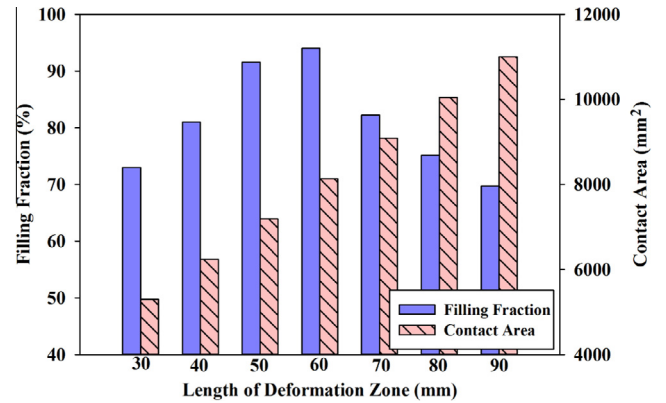


Fig. 13. Effect of  $L_{DZ}$  on the filling fraction of the die at a constant  $D_R$  of 2.

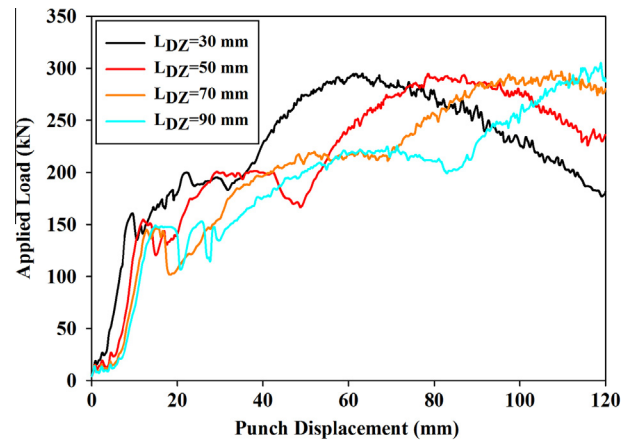


Fig. 14. Effect of  $L_{DZ}$  on the pressing load at constant  $D_R$  of 2.

In fact, the real contact area between the die walls and the deforming sample is a function of filling fraction which has increased up to  $L_{DZ} = 60$  mm and afterwards, it has decreased. Therefore, although the surface area of the deformation zone is increased by  $L_{DZ}$ ,

however, the real frictional contact area between the die walls and the deforming sample is not necessarily increased and therefore, reduction in pressing load is expected for  $L_{DZ}$  larger than 60 mm. In the cases of  $L_{DZ}$  smaller than 60 mm in which both  $L_{DZ}$  and filling fraction (consequently the contact surface) are increasing by increasing  $L_{DZ}$ , it may be stated that the rate of increase in pressing load caused by increased contact frictional surface is less than the rate of decrease in the deformation load caused by reduction in the imposed strain. Therefore, the pressing load is in overall reducing by increasing  $L_{DZ}$ .

## 6. Conclusions

In the present paper, influence of the die design parameters on the deformation in pure shear extrusion (PSE) is investigated. Computer simulation of the process is performed with the help of Deform-3D™ FEM commercial package. According to the results of this investigation, the following conclusions are made;

- (1) Variation of pressing load versus punch displacement in experiments is analyzed. Six different regions are observed in the pressing load graph which are related to the material movement in different zones of the die. In addition, changes in the geometry of the work-piece before entering into, inside and after exiting the deformation zone are illustrated. It is observed that the deforming work-piece would not fully fill in the die channel and corner gaps are formed.
- (2) Predicted pressing load versus punch displacement and filling fraction of the die exit channel at various shear friction coefficient ( $m$ ) are compared with the experimental results to verify the predictions of simulation. It is observed that a good agreement between predictions of simulation and the experimental results is found at  $m = 0.4$ . In addition, color coded microhardness map is compared to the effective strain map contour which indicates a good agreement.
- (3) Effective strain, inhomogeneity of strain, pressing load and filling fraction of the die exit channel are increased with increasing diameter ratio. In fact, by enhancement of the diameter ratio, the work-piece is forced to deform in a narrower deformation zone and larger strain is imposed and consequently, the inhomogeneity increases. In addition, as the diameter ratio increases, further deformation is applied and frictional contact area increases which result in higher pressing load. Therefore, backward pressure as a function of pressing load increases as well and higher filling fraction of the die exit channel is obtained. According to the results of this investigation, the optimum proposed value for diameter ratio is 2.
- (4) By enhancement of the length of deformation zone, pressing load and effective strain gradually decreases and the difference between the amount of deformation in peripheral and central regions reduces. In fact, the work-piece is deformed more homogeneously at lower pressing load. However, filling fraction of the die exit channel increases to an optimum value, i.e., 60 mm, after which it decreases. By increasing length of deformation zone, the work-piece is deformed in a larger region with in less frictional contact area which results in lower pressing load.

